Electrochemical Switching of Photoelectrochemical Processes at CdS QDs and Photosystem I-Modified Electrodes

Ariel Efrati,[‡] Omer Yehezkeli,[†] Ran Tel-Vered,[†] Dorit Michaeli,[‡] Rachel Nechushtai,[‡] and Itamar Willner[†,*]

[†]The Minerva Center for Biohybrid Systems, Institute of Chemistry, The Hebrew University of Jerusalem, Jerusalem 91904, Israel and [‡]Department of Plant Sciences, The Alexander Silberman Institute of Life Sciences, The Hebrew University of Jerusalem, Jerusalem 91904, Israel

ABSTRACT

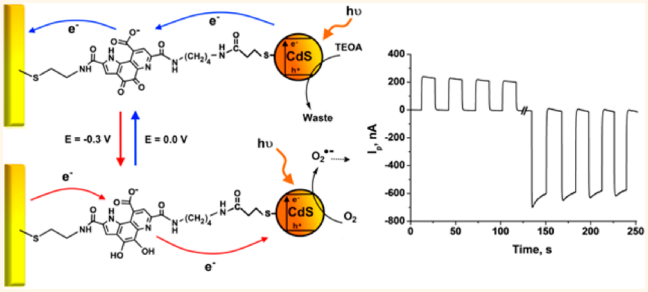

Photoactive inorganic CdS quantum dots (QDs) or the native photosystem I (PSI) is immobilized onto a pyrroloquinoline quinone (PQQ) monolayer linked to Au electrodes to yield hybrid relay/QDs (or photosystem) assemblies. By the electrochemical biasing of the electrode potential, the relay units are retained in their oxidized PQQ or reduced $PQQH_2$ states. The oxidized or reduced states of the relay units dictate the direction of the photocurrent (anodic or cathodic). By the cyclic biasing of the electrode potential between the values $E \geq -0.05$ V and $E \leq -0.3$ V *vs* Ag quasi-reference electrode (Ag QRE), retaining the relay units in the oxidized PQQ or reduced $PQQH_2$ states, the photocurrents are respectively switched between anodic and cathodic values. Different configurations of electrically switchable photoelectrochemical systems are described: (i) the PQQ/CdS QDs/(triethanolamine, TEOA) or PQQ/PSI/(ascorbic acid/dichlorophenolindophenol, DCPIP) systems, leading to anodic photocurrents; (ii) the PQQ/CdS QDs (or PSI)/(flavin adenine dinucleotide) systems, leading to cathodic photocurrents; (iii) the PQQ/CdS QDs (or PSI)/(O_2) switchable systems, leading to cyclic anodic/cathodic switching of the photocurrents.

KEYWORDS: photoelectrochemistry · electrochemical switching · quantum dots · switch · photosystem · photocurrent · modified electrode

The signal-controlled, switchable, charge transport at chemically modified electrode surfaces attracts substantial research efforts directed to the development of nanoscale molecular electronic devices,[1−5] the design of information storage and processing systems,[6−8] the development of molecular machines,[9−12] the fabrication of surfaces of controllable wettabilities,[13−16] the controlled uptake/release of substrates,[17−19] and the assembly of sensor[20,21] or biosensor systems.[22] Different stimuli were implemented to switch the charge transport properties at electrode surfaces, and these included photonic,[23,24] electrical,[25] magnetic,[26−28] thermal,[29] pH,[30,31] or chemical (*e.g.*, redox processes, DNA strands)[32] signals. The functionalization of electrodes with supramolecular photoactive molecular nanostructures, or semiconductor nanoparticles (quantum dots, QDs), enabled the development of photoelectrochemical systems revealing vectorial electron transfer,[33] systems exhibiting ON/OFF photoswitchable generation of photocurrents,[34] and photoelectrochemical systems triggered by external stimuli to yield dictated directions of photocurrents (cathodic or anodic).[35,36] For example, by the tethering of photosensitizer units to helical peptides associated with electrodes, photodiodes that switch the direction of photocurrents were demonstrated,[37] and by the use of a diffusional quasi-reversible redox couple ($Fe(CN)_6^{3-/4-}$), the potential-assisted control of photocurrents generated by a PSI-modified electrode was reported.[38] Similarly, the organization of electron-acceptor/photosensitizer[39,40] or electron-acceptor/QDs[41] nanostructures on electrode surfaces enabled the enhancement of cathodic photocurrents upon photoirradiation of the light-active components. Also, the nanoengineering of photosensitizers (or QDs) and electron acceptors on DNA scaffolds associated with electrodes enabled the design of photoelectrochemical systems, revealing dictated anodic or cathodic photocurrents.[42] Furthermore, the chemically-induced formation of hemin/G-quadruplexes on semiconductor QDs associated with electrodes enabled the catalyzed

* Address correspondence to willnea@vms.huji.ac.il.

Received for review August 16, 2012 and accepted September 25, 2012.

Published online September 25, 2012
10.1021/nn3037286

generation of chemiluminescence and the subsequent chemiluminescence resonance energy transfer to the QDs, leading to the generation of anodic photocurrents without external irradiation.[43] The switchable generation of photocurrents was demonstrated, for example, by the integration of semiconductor QDs with polymer matrices undergoing reversible gel-to-solid phase transitions in the presence of external stimuli.[44] The voltage-stimulated switching of the direction of photocurrents was demonstrated by designing molecular assemblies on electrodes and using dye molecules or QDs as photoactive units, in the presence of solubilized donor or acceptor molecules. For example, the intercalation of methylene blue into a CdS-functionalized DNA duplex allowed the potential-induced switching of the photocurrent between anodic or cathodic directions, upon oxidation or reduction of the intercalated units, respectively.[45]

In the present study we report on the modification of electrodes with photosensitizer/relay assemblies, and we demonstrate the potential-induced control of the directions of the photocurrents in the systems. The different assemblies implement CdS quantum dots or the native photosystem I (PSI) as the photoactive component, and pyrroloquinoline quinone, PQQ (**1**), is used as a mediating redox relay unit.

RESULTS AND DISCUSSION

Pyrroloquinoline quinone, covalently bound to a Au electrode, exhibits a redox wave at *ca.* $E = -0.08$ V *vs* a Ag quasi-reference wire electrode (Ag QRE), Figure S1, Supporting Information. This biological electroactive substrate was extensively used as a redox relay for the activation of bioelectrocataltyic processes.[46] PQQ (**1**) was covalently linked to a cysteamine monolayer-modified electrode (surface coverage of PQQ, 2.6×10^{-10} mol·cm^{-2}). The resulting monolayer was reacted with 1,4-diaminobutane, and subsequently, mercaptopropionic acid-modified CdS QDs (*ca.* 6 nm) were covalently linked to the resulting monolayer. The surface coverage of the CdS QDs was determined by quartz crystal microbalance, QCM, and by complementary grazing angle XPS measurements to be *ca.* 1.7×10^{12} NPs·cm^{-2}.

In the first phase of the study, we have examined possibilities to dictate the directions of the photocurrents generated by the CdS QDs-modified electrodes by means of the constituents of the systems and the bias potential applied on the electrodes. In one system, Figure 1A, the PQQ/CdS QDs-functionalized electrode was irradiated under Ar in the presence of triethanolamine, TEOA, as a sacrificial electron donor. Under open-circuit voltage, illumination of the electrode results in the photocurrent action spectrum shown in Figure 1B. The photocurrent spectrum follows the absorption characteristics of the CdS QDs, implying that the photoexcitation of the QDs is the origin of the photocurrent. Control experiments reveal that upon exclusion of TEOA from the system, no photocurrent is generated. Also, the direct coupling of the CdS QDs to the cysteamine monolayer (in the absence of the PQQ), and in the presence of TEOA, results in a *ca.* 10-fold lower photocurrent as compared to the PQQ/CdS QDs system. Figure 1C depicts the effect of applied potential on the photocurrent generated upon irradiation of the PQQ/CdS QDs electrode. At a positive potential, $E = 0.2$ V *vs* Ag QRE, an anodic photocurrent of *ca.* 700 nA is observed. As the potential is negatively shifted, the intensities of the photocurrents decrease, and the photocurrent is being fully blocked at bias potentials lower than $E = -0.3$ V *vs* Ag QRE. Evidently, a sharp decline in the photocurrent is observed at *ca.* $E = -0.1$ V, close to the redox potential of the PQQ relay units. These results are consistent with the mechanism outlined in Figure 1A. Photoexcitation of the CdS QDs results in the formation of an electron–hole pair. As the electrode is biased at positive potentials, the electron transfer of the QDs' conduction-band electrons ($V_{CB} = -1.14$ V *vs* SCE)[45] to the PQQ units results in the charge separation of the electron–hole pair. The subsequent oxidation of the sacrificial electron donor, TEOA, and the transfer of electrons from the reduced PQQ units to the electrode lead, then, to a steady-state anodic photocurrent. At potentials lower than $E = -0.2$ V, the relay units exist in the reduced $PQQH_2$ state. This eliminates the trapping of the conduction-band electrons and the subsequent charge separation of the electron–hole pair. Thus, the spatial separation of the CdS QDs from the electrode and the competitive electron–hole recombination prohibit the formation of a photocurrent. The cyclic ON/OFF irradiation of the electrode at a potential corresponding to $E = 0.0$ V *vs* Ag QRE results in the reversible switching of the anodic photocurrent between "ON" and "OFF" states, Figure 1D. In the second system, Figure 1E, the sacrificial electron donor, TEOA, is excluded from the system, and the electron acceptor flavin adenine dinucleotide, FAD, is added as a constituent. Upon biasing the electrode at $E = -0.3$ V, the PQQ relay units exist in their reduced sate, $PQQH_2$, exhibiting electron-donor properties. Irradiation of the system under argon, and upon biasing the electrode at $E = -0.3$ V, results in the formation of a cathodic photocurrent. Also, control experiments revealed that upon biasing the electrode potential at values positive to $E = 0.0$ V, the cathodic photocurrent is fully blocked. By subjecting the electrode to the cyclic switchable illumination, at $E = -0.3$ V, the light-modulated reversible ON/OFF switching of the cathodic photocurrent was observed, Figure 1F. The formation of the cathodic photocurrent is rationalized in terms of the electron transfer reactions outlined in Figure 1E. Photoexcitation of the CdS QDs yields the respective electron–hole pair. As the electrode is biased at $E = -0.3$ V, the relay units exist in

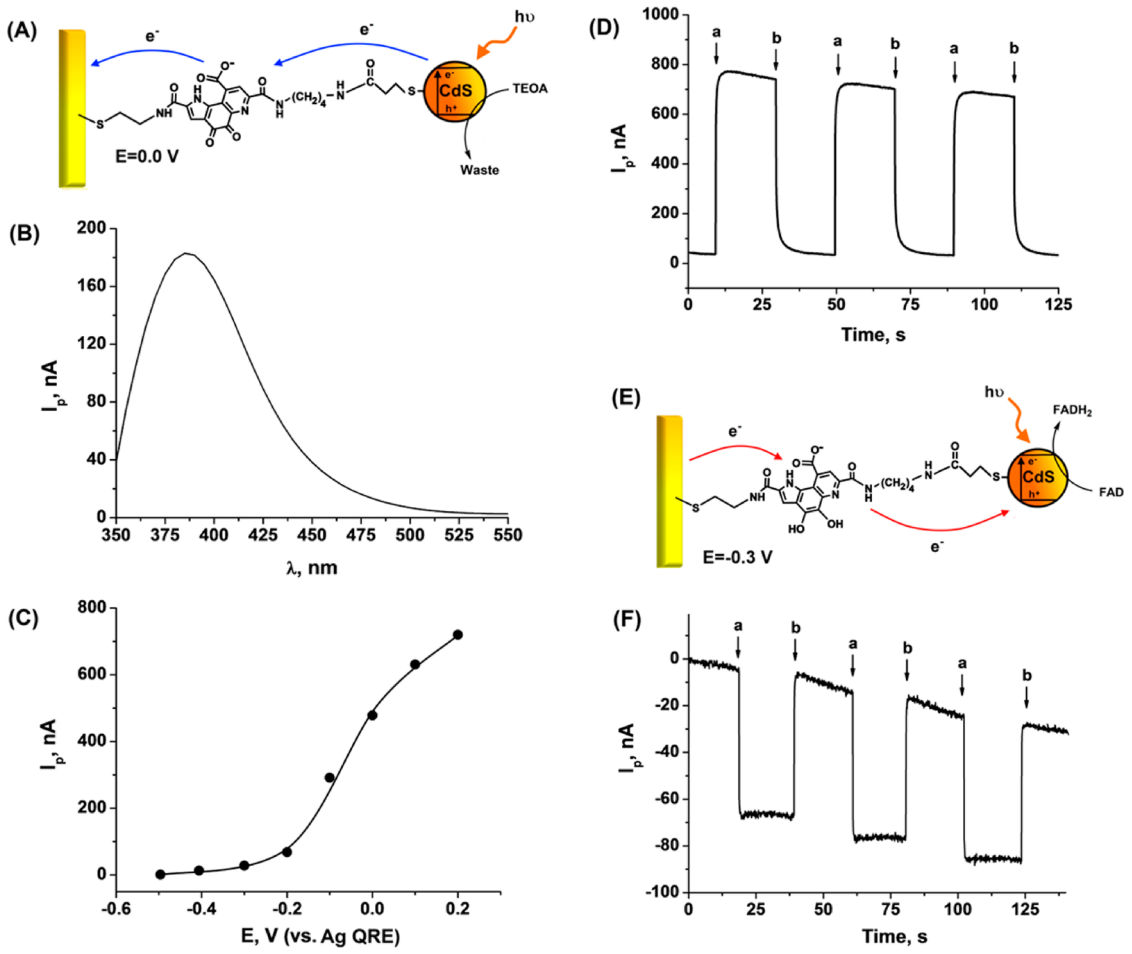

Figure 1. (A) Schematic presentation for the generation of an anodic photocurrent on a PQQ/CdS QDs-modified electrode, under Ar, and in the presence of TEOA. Applied bias potential, E = 0.0 V *vs* Ag QRE. (B) Photocurrent action spectrum corresponding to the PQQ/CdS QDs-modified electrode, under Ar, and in the presence of TEOA, 40 mM. The spectrum is recorded at open-circuit potential. (C) Effect of applied bias potential on the photocurrent intensity, at λ = 380 nm, corresponding to the PQQ/CdS QDs-modified electrode, under Ar, and in the presence of TEOA, 40 mM. (D) Photocurrent responses, at λ = 380 nm, upon the cyclic switchable illumination of the PQQ/CdS QDs-modified electrode, at E = 0.0 V *vs* Ag QRE, under Ar, and in the presence of TEOA, 40 mM. Switch "ON" (illumination on)-marked (a); switch "OFF"-marked (b). (E) Schematic presentation for the generation of a cathodic photocurrent on a PQQ/CdS QDs-modified electrode, under Ar, and in the presence of FAD. Applied bias potential, E = −0.3 V *vs* Ag QRE. (F) Photocurrent responses, at λ = 380 nm, upon the cyclic switchable illumination of the PQQ/CdS QDs-modified electrode, at E = −0.3 V *vs* Ag QRE, under Ar, and in the presence of FAD, 140 μM. Switch "ON" (illumination on)-marked (a); switch "OFF"-marked (b). All measurements were performed in a phosphate buffer (0.1 M, pH = 8.0); effective electrode surface area 0.25 cm^2.

their reduced, electron-donating state, $PQQH_2$. The transfer of electrons from the reduced relays to the valence-band holes, and the concomitant transfer of the conduction-band electrons to the FAD electron-acceptor units, result in the steady-state cathodic current observed. It should be noted that the cathodic currents are substantially lower than the anodic currents that are obtained in the presence of TEOA. This may be attributed to the following reasons: (i) The relatively higher concentration of TEOA and its sacrificial oxidation by the valence band holes effectively deplete the holes, thus competing effectively with the electron−hole recombination process. (ii) The absorbance of the FAD component overlaps the spectrum of the CdS QDs, thus leading to the lower currents.

We have, then, implemented the natural photosynthetic reaction center, photosystem I, which was extracted from the thermophilic cyanobacterium *Mastigocladus laminsus*, as the light-active component to photostimulate the directional switching of photocurrents at chemically-modified electrodes. The generation of photocurrents by quinone/PSI monolayer-[47,48] or by bis-aniline-cross-linked Pt nanoparticles/PSI-functionalized electrodes was previously demonstrated,[49] but the effects of biased potential on the intensities and directions of the photocurrents integrated electrodes were not examined. Accordingly, a PQQ/PSI-modified electrode, Figure 2A, was assembled by the primary modification of the cysteamine-modified Au electrode with the PQQ units, followed by the covalent attachment of PSI to the electrode,

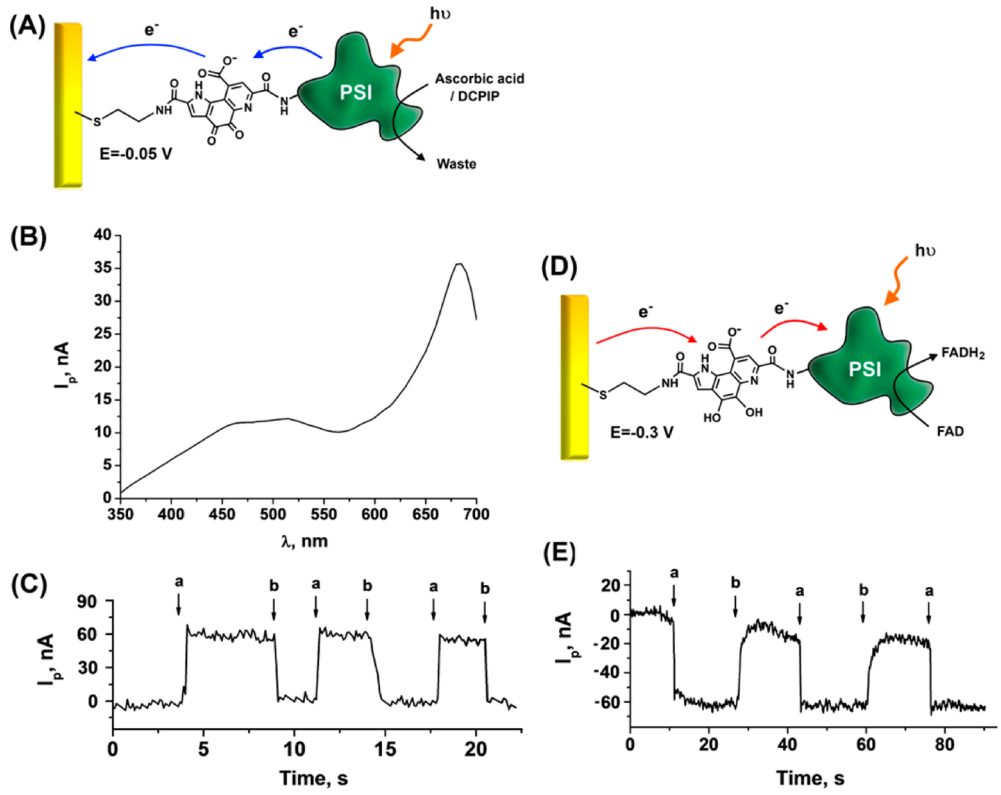

Figure 2. (A) Schematic presentation for the generation of an anodic photocurrent on a PQQ/PSI-modified electrode, under Ar and in the presence of ascorbic acid/DCPIP. Applied bias potential, $E = -0.05$ V *vs* Ag QRE. (B) Photocurrent action spectrum corresponding to the PQQ/PSI-modified electrode, under Ar and in the presence of DCPIP, 62 μM, and ascorbic acid, 40 mM. The spectrum is recorded at open-circuit potential. (C) Photocurrent responses, at $\lambda = 680$ nm, upon the cyclic switchable illumination of the PQQ/PSI-modified electrode, at $E = -0.05$ V *vs* Ag QRE, under Ar, and in the presence of DCPIP, 62 μM, and ascorbic acid, 40 mM. Switch "ON" (illumination on)-marked (a); switch "OFF"-marked (b). (D) Schematic presentation for the generation of a cathodic photocurrent on a PQQ/PSI-modified electrode, under Ar, and in the presence of FAD. Applied bias potential, $E = -0.3$ V *vs* Ag QRE. (E) Photocurrent responses, at $\lambda = 680$ nm, upon the cyclic switchable illumination of the PQQ/PSI-modified electrode, at $E = -0.3$ V *vs* Ag QRE, under Ar, and in the presence of FAD, 140 μM. Switch "ON" (illumination on)-marked (a); switch "OFF"-marked (b). All measurements were performed in a phosphate buffer (0.1 M, pH = 8.0); effective electrode surface area 0.25 cm^2.

through the lysine amino acids existing in the protein backbone. Complementary QCM measurements indicated that the surface coverage of PSI corresponded to 6.6×10^{-13} mol·cm^{-2}. Irradiation of the electrode, under argon, at open-circuit voltage and in the presence of ascorbic acid/dichlorophenolindophenol, DCPIP, as an electron-donating system, resulted in the anodic photocurrent spectrum shown in Figure 2B. The photocurrent spectrum follows the absorption pattern of PSI and is very similar to the photocurrent spectra of PSI/ascorbic acid-DCPIP observed in other systems.[50] Control experiments revealed that no photocurrents were formed in the absence of ascorbic acid/DCPIP and that the direct immobilization of PSI on the electrode generated very low photocurrents in the presence of the electron-donor system. Also, biasing the potential at $E = -0.3$ V *vs* Ag QRE blocked the photocurrent generated by the electrode. These results indicate that the PQQ/PSI hybrid assembled on the electrode allows the generation of an anodic current, upon biasing the electrode at a potential corresponding to $E > E^{o}_{PQQ}$ (at pH = 8.0), which retains the PQQ relay units in their oxidized state. That is, electron transfer from the P_{700} unit of the photoexcited PSI to the PQQ relay units leads to charge separation. The subsequent reduction of the oxidized P_{700}^{+} center of PSI by the ascorbic acid/DCPIP and the concomitant electron transfer of the electrons from the relay units to the electrode result in the generation of the anodic photocurrent. The light-modulated ON/OFF switching of the anodic photocurrents, upon the application of cyclic ON/OFF irradiation of the electrode, at $E = -0.05$ V *vs* Ag QRE, is presented in Figure 2C. Evidently, anodic photocurrents of *ca.* 60 nA were repeatedly switched ON and OFF, using the intermittent illumination at $\lambda = 680$ nm.

The PSI-induced generation of cathodic photocurrents is schematically depicted in Figure 2D. The electron-donating component, ascorbic acid/DCPIP, is excluded from the system, and flavin adenine dinucleotide is added as an electron acceptor. Irradiation of the PQQ/PSI-functionalized electrode under Ar and biasing the electrode potential at $E = -0.3$ V *vs* Ag QRE, result in the formation of a cathodic photocurrent.

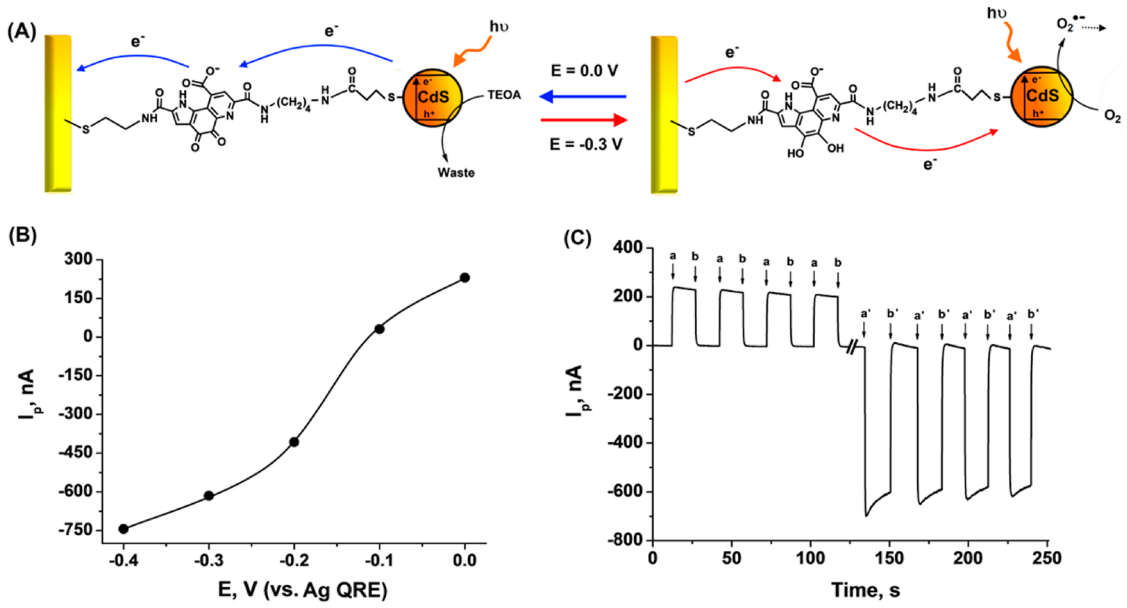

Figure 3. (A) Potential-induced control of photocurrent directionality (anodic or cathodic) on a PQQ/CdS QDs-modified electrode, under O_2, and in the presence of TEOA. (B) Effect of applied bias potential on the photocurrent intensity, at λ = 380 nm, corresponding to the PQQ/CdS QDs-modified electrode, under O_2, and in the presence of TEOA, 40 mM. (C) Photocurrent responses, at λ = 380 nm, upon the cyclic switchable illumination of the PQQ/CdS QDs-modified electrode, under O_2, and in the presence of TEOA, 40 mM. (a) Illumination on, E = 0.0 V *vs* Ag QRE, (b) illumination off, E = 0.0 V. (a′) Illumination on, E = −0.3 V *vs* Ag QRE, (b′) illumination off, E = −0.3 V. All measurements were performed in a phosphate buffer (0.1 M, pH = 8.0); effective electrode surface area 0.25 cm^2.

Control experiments indicated that no photocurrent is generated when the electrode is biased at E = 0.0 V *vs* Ag QRE, implying that the relay units must exist in their reduced $PQQH_2$ state. Also, no photocurrent was observed under Ar, at E = −0.3 V, upon exclusion of the FAD from the system. Accordingly, the cathodic photocurrent originates from the photoexcitation of PSI and the electron transfer to the FAD electron acceptor. The subsequent reduction of the oxidized P_{700}^+ site by $PQQH_2$ regenerates the photosystem while generating a steady-state cathodic photocurrent. Indeed, upon the cyclic switching of the illumination on the electrode, at E = −0.3 V, the cathodic photocurrent generated by the PQQ/PSI-modified electrode was reversibly switched between the ON and OFF states, Figure 2E.

The systems described in Figures 1 and 2 demonstrated that by changing the constituents of the systems and by controlling the bias potential on the PQQ/CdS QDs- or PQQ/PSI-modified electrodes the directions of the photocurrent (anodic or cathodic) could be controlled. Nonetheless, these systems did not enable the construction of integrated devices that could be switched repeatedly between anodic and cathodic photocurrents through biasing the electrode potential (and controlling the redox state of the relay units PQQ/$PQQH_2$). This difficulty is mainly due to the fact that the ascorbic acid/DCPIP/FAD and the TEOA/FAD couples exhibit their own photochemical reactions that perturb the specific interactions with the photoactive electrodes generating the photocurrents. To overcome these difficulties, we made use of the fact that oxygen (O_2) acts as an electron acceptor for the conduction-band electrons generated in the CdS QDs and its ability to quench, *via* electron transfer, the photoexcited PSI.[51,52] Thus, we examined the effect of biasing the potential of the PQQ/CdS QDs-functionalized electrode, upon its irradiation under oxygen, and in the presence of triethanolamine as an electron donor, Figure 3A. The photocurrents generated by the modified electrode at different bias potentials are depicted in Figure 3B. At a bias potential of E = 0.0 V *vs* Ag QRE, an anodic photocurrent is observed (*ca.* 220 nA), and a further negative shift of the potential decreases the photocurrent to zero, at *ca.* E = −0.1 V. Shifting the potentials to more negative values yields a cathodic photocurrent that reaches a value of *ca.* 750 nA at E = −0.4 V. These results can be rationalized in terms of the functions of the PQQ relay units in controlling the directions of the photocurrents. At E = 0.0 V, the relay units exist in the oxidized PQQ state. This results in the transfer of the photoexcited conduction band electrons to the PQQ units. The subsequent scavenging of the valence band holes by triethanolamine, and the concomitant potential-assisted transfer of the electrons to the electrode lead to the formation of a steady-state anodic photocurrent. At potentials lower than −0.10 V, the relay groups exist in their reduced $PQQH_2$ state, and consequently, the trapping of the conduction-band electrons and the subsequent charge separation are prohibited. Under these conditions, the alternative mechanism leading to the cathodic photocurrent is activated. Oxygen acts as an electron acceptor for

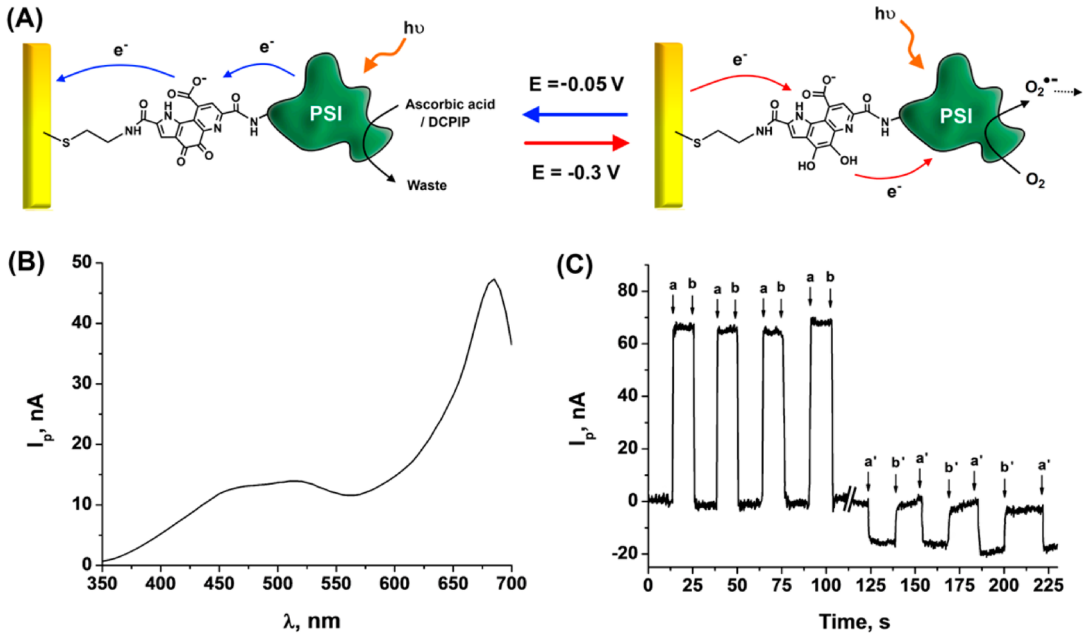

Figure 4. (A) Potential-induced control of photocurrent directionality (anodic or cathodic) on a PQQ/PSI-modified electrode, under O_2, and in the presence of ascorbic acid/DCPIP. (B) Photocurrent action spectrum corresponding to the PQQ/PSI-modified electrode, under O_2, and in the presence of DCPIP, 62 μM, and ascorbic acid, 40 mM. The spectrum is recorded at open-circuit potential. (C) Photocurrent responses, at λ = 680 nm, upon the cyclic switchable illumination of the PQQ/PSI-modified electrode, under O_2, and in the presence of DCPIP, 62 μM, and ascorbic acid, 40 mM. (a) Illumination on, $E = -0.05$ V *vs* Ag QRE, (b) illumination off, $E = -0.05$ V. (a′) Illumination on, $E = -0.3$ V *vs* Ag QRE, (b′) illumination off, $E = -0.3$ V. All measurements were performed in a phosphate buffer (0.1 M, pH = 8.0); effective electrode surface area 0.25 cm^2.

the photoexcited conduction-band electrons, and the reduced relay units provide the electrons to reduce the holes at the valence band. As the electrode is biased at $E < -0.1$ V, the relay units are retained in their reduced state, $PQQH_2$, leading to a steady-state cathodic current. At the bias potential of *ca.* $E = -0.1$ V, no net photocurrent is generated. This is the redox potential of the PQQ/$PQQH_2$ relay units. That is, at this potential the populations of PQQ and $PQQH_2$ are almost identical, leading to the generation of photocurrents exhibiting opposite directions and, thus, to a net zero photocurrent. Furthermore, it should be noted that the PQQ/CdS QDs-modified electrode generates, upon the application of the bias potential of $E = 0.0$ V, a lower anodic photocurrent under oxygen (*ca.* 220 nA) as compared to the photocurrent generated by the electrode subjected to a similar potential and irradiated under Ar (*ca.* 500 nA, cf. Figure 1C). These results are consistent with the fact that under oxygen the non-photocurrent-generating path, where the oxygen acts as an acceptor and TEOA acts as a donor, competes with the route of the anodic photocurrent generation, and thus, its net value is lower. Using cyclic switchable illumination and by the application of the potentials 0.0 and −0.3 V on the PQQ/CdS QDs-modified electrode, the ON/OFF switching of the anodic and the cathodic photocurrents is respectively demonstrated, Figure 3C.

Similarly, the PQQ/PSI system has been implemented as an integrated assembly for the potential-stimulated cyclic control of anodic and cathodic photocurrents by the irradiation of the modified electrode under oxygen, Figure 4. Upon the application of a bias potential corresponding to $E = -0.05$ V *vs* Ag QRE that retains the relay units in their oxidized PQQ state, and the irradiation of the functionalized electrode under O_2, in the presence of ascorbic acid/DCPIP, an anodic photocurrent is generated. Figure 4B depicts the photocurrent spectrum that follows the absorption pattern of PSI. Switching the bias potential on the electrode to $E = -0.3$ V, a potential that retains the relay units in their reduced $PQQH_2$ state, yields, upon irradiation under O_2, a cathodic photocurrent. This is attributed to the electron transfer quenching of the excited PSI by O_2 and the subsequent reduction of the resulting P_{700}^+ by the $PQQH_2$ units. Control experiments reveal that the direct immobilization of PSI onto the electrode (without PQQ) does not lead to any anodic photocurrent in the presence of ascorbic acid/DCPIP (at $E = -0.05$ V). Similarly, a minute cathodic photocurrent is observed in the PQQ/PSI system upon exclusion of O_2 (at $E = -0.3$ V). These control experiments imply that the PQQ is, indeed, an essential component for electrically wiring PSI with the electrode and that the added O_2 leads to the generation of resulting cathodic photocurrent. Subjecting the electrode to cyclic ON/OFF irradiation, and by applying the potentials $E = -0.05$ V and $E = -0.3$ V in the presence of O_2, anodic and cathodic photocurrents were respectively generated by the PQQ/PSI system, Figure 4C. It should be noted that in all of the PSI-functionalized

electrodes described in our study the PSI is not oriented on the electrode surface due to the random attachment of the different lysine residues to the PQQ relay units. The PQQ units are electrically wiring the PSI units to the electrode, and, naturally, the wiring efficiencies differ with respect to the different orientations of the PSI proteins. Thus, the resulting anodic/cathodic currents represent the average result of all different electrically wired PSI configurations. Furthermore, it should be noted that the potential-induced anodic/cathodic photocurrents generated by the PQQ/CdS QDs/O_2 system, Figure 3, are substantially higher (*ca.* 12-fold) compared to the analogous PQQ/PSI/O_2 system. Taking into account the surface coverage of the PSI and CdS QDs systems on the electrodes and the overall number of photons absorbed by the two photoactive systems, only a 7-fold enhancement in the photocurrent generated by the CdS QDs system is anticipated. The observed 12-fold-enhanced photocurrent generated by the CdS QDs, as compared to the PSI assembly, is attributed to a lower performance of the PSI system in generating the photocurrent. The lower photocurrent yields in the PQQ/PSI/O_2 system are attributed to the random configurations of the photoactive centers and to the protein shell surrounding the photoactive centers that perturbs the electrical contacting of the PSI photocenters with the electrodes by the PQQ relay units.[53] Such orientation effects or barriers for the electron transfer do not exist in the spherical monolayer-capped QDs.

CONCLUSIONS

In conclusion, the present study has demonstrated the integration of semiconductor CdS QDs and the native PSI as photoactive materials with electrodes, and the potential-induced control of the directions of the resulting photocurrents in the systems. The comparison between the PSI and the CdS QDs systems should be considered, however, with caution. The footprint areas of the PSI[54,55] and CdS QDs differ substantially, 330 *vs ca.* 110 nm^2, respectively, and the electrical communication of PSI with the electrode by the PQQ relay units suffers from orientation and protein-insulating effects that do not exist in the QDs system. Thus, the two systems reveal only functional similarities, and hence, any comparison should be considered as qualitative rather than quantitative. We demonstrated that the implementation of the common pyrroloquinoline quinone, as a relay unit, enabled the potential-assisted control of the photoelectrochemical systems. Specifically, we demonstrated the assembly of integrated PQQ/CdS QDs or PQQ/PSI systems that, upon irradiation under O_2, lead to potential-triggered photodiodes, resulting in photocurrents of switchable anodic and cathodic directions. The successful assembly of optoelectronic photodiode systems based on inorganic QDs and the PSI biomaterial bridges the boundaries between supramolecular chemistry, nanotechnology, and nanobiotechnology.

MATERIALS AND METHODS

Materials. Ultrapure water from a NANOpure Diamond (Barnstead) source was used throughout the experiments. Pyrroloquinoline quinone was obtained from Fluka; triethanolamine was obtained from Aldrich. Ascorbic acid, sodium 2,6-dichloroindophenolate hydrate, and flavin adenine dinucleotide disodium salt were obtained from Sigma. Photosystem I was extracted from the thermophilic cyanobacterium *Mastigocladus laminsus* and purified according to a previously reported procedure.[56]

CdS QDs were synthesized according to the following procedure: a dioctyl sulfosuccinate sodium salt, AOT/*n*-heptane water-in-oil microemulsion, was prepared by the solubilization of 3.5 mL of distilled water in 100 mL of *n*-heptane in the presence of AOT as a surfactant. The resulting mixture was separated into 60 and 40 μL subvolumes. An aqueous solution of $Cd(ClO_4)_2$ (240 μL, 1.55 M) and Na_2S (160 μL, 1.32 M) was added to the 60 and 40 μL subvolumes, respectively. The two subvolumes were then mixed and stirred for 1 h to yield the NPs. For the preparation of thiol-capped CdS QDs, mercaptoethyl sulfonate (20 mg) and mercaptopropionic acid (3.3 mg) were added to the resulting micellar solution, and the mixture was stirred for 14 h under argon. Pyridine, 20 mL, was then added, and the resulting precipitate was washed and centrifuged with *n*-heptane, petroleum ether, butanol, and methanol. An average particle size of 6.0 $\pm$ 0.5 nm was estimated by TEM.

Modification of the Electrodes. Clean Au slides were reacted for 6 h with an aqueous solution of cysteamine, 10 mM. The resulting cysteamine monolayer-modified electrodes were treated for 2 h with a 3 mL HEPES buffer solution (50 mM, pH = 7.2) that included 1 mg of PQQ dissolved in 50 μL of DMSO and 5 mM 1-(3-dimethylaminoproyl)-3-ethylcarbodiimide hydrochloride (EDC) and *N*-hydroxysulfosuccinimide sodium salt (NHS). For the preparation of the PSI-functionalized electrodes, the PQQ-modified electrodes were then reacted for 2 h with a HEPES buffer solution (50 mM, pH = 7.2) that contained 2 mg of Chl mL^{-1} PSI and 5 mM EDC/NHS. For the preparation of the CdS QDs-functionalized electrodes, the PQQ-modified electrodes were treated for 2 h with a HEPES buffer solution (50 mM, pH = 7.2) that contained 5 mg mL^{-1} 1,4-diaminobutane and 5 mM EDC/NHS. The resulting electrodes were then treated with a HEPES buffer solution (50 mM, pH = 7.2) that contained 1 mg mL^{-1} mercaptopropionic acid-modified CdS QDs. Following the modifications, the electrodes were rinsed with a HEPES buffer solution to remove any nonspecifically bound reagents.

Measurements and Instrumentation. Photoelectrochemical measurements were performed using a home-built system that included a Xe lamp (Oriel, model 6258, $P_{380\ nm}$ = 500 μW and $P_{680\ nm}$ = 70 μW), a monochromator (Oriel, model 74000, 2 nm resolution), and a chopper (Oriel, model 76994). The electrical output from the cell was sampled by a lock-in amplifier (Stanford Research, model SR 830 DSP). The shutter chopping frequency was controlled by a Stanford Research pulse/delay generator, model DE535. The photogenerated currents were measured between the modified working electrodes and a Pt plate counter electrode. In all photoelectrochemical experiments the effective electrode surface area corresponded to 0.25 cm^2. In some experiments, an Autolab potentiostat (ECO Chemie, The Netherlands) driven by GPES software was coupled to the photoelectrochemical apparatus, allowing the measurement of the photocurrents upon the application of different external potentials on the modified electrodes. In these

experiments, a Ag wire ($d = 0.5$ mm) and a carbon rod ($d = 5$ mm) or a Pt slide were used as the reference and counter electrodes, respectively, and the values reported represent the difference between the currents measured under illumination and in the dark. In all photocurrent switching experiments, the current responses, in the dark, were normalized to zero. QCM measurements were performed using a home-built instrument linked to a frequency analyzer (Fluke) using Au-quartz crystals (AT-cut, 10 MHz).

Conflict of Interest: The authors declare no competing financial interest.

Supporting Information Available: Cyclic voltammograms of the PQQ-modified Au electrode at variable scan rates and the dependence of the peak anodic current on the scan rate are presented. This material is available free of charge *via* the Internet at http://pubs.acs.org.

Acknowledgment. This research is supported by the NanoSensoMach ERC Advanced Grant No. 267574 under the EC FP7/2007-2013 program.

REFERENCES AND NOTES

1. Coskun, A.; Spruell, J. M.; Barin, G.; Dichtel, W. R.; Flood, A. H.; Botros, Y. Y.; Stoddart, J. F. High Hopes: Can Molecular Electronics Realise its Potential? *Chem. Soc. Rev.* **2012**, *41*, 4827–4859.
2. Saha, S.; Johansson, E.; Flood, A. H.; Tseng, H.-R.; Zink, J. I.; Stoddart, J. F. A Photoactive Molecular Triad as a Nanoscale Power Supply for a Supramolecular Machine. *Chem.—Eur. J.* **2005**, *11*, 6846–6858.
3. Willner, I. Photoswitchable Biomaterials: En Route to Optobioelectronic Systems. *Acc. Chem. Res.* **1997**, *30*, 347–356.
4. Jager, E. W. H.; Smela, E.; Inganäs, O. Microfabricating Conjugated Polymer Actuators. *Science* **2000**, *290*, 1540–1545.
5. Fox., M. A. Fundamentals in the Design of Molecular Electronic Devices: Long-Range Charge Carrier Transport and Electronic Coupling. *Acc. Chem. Res.* **1999**, *32*, 201–207.
6. Liu, Z. F.; Hashimoto, K.; Fujishima, A. Photoelectrochemical Information Storage Using an Azobenzene Derivative. *Nature* **1990**, *347*, 658–660.
7. Green, E. J.; Choi, W. J.; Boukai, A.; Bunimovich, Y.; Johanston-Halperin, E.; Delonno, E.; Lou, Y.; Sheriff, B. A.; Xu, K.; Shin, S. Y.; *et al.* A 160-Kilobit Molecular Electronic Memory Patterned at 10^{11} Bits per Square Centimeter. *Nature* **2007**, *445*, 414–417.
8. Baron, R.; Onopriyenko, A.; Katz, E.; Lioubashevski, O.; Willner, I.; Wang, S.; Tian, H. An Electrochemical/Photochemical Information Processing System Using a Monolayer-Functionalized Electrode. *Chem. Commun.* **2006**, 2147–2149.
9. Yang, W.; Li, Y.; Liu, H.; Chi, L.; Li, Y. Design and Assembly of Rotaxane-Based Molecular Switches and Machines. *Small* **2012**, *8*, 504–516.
10. Katz, E.; Lioubashevski, O.; Willner, I. Electromechanics of a Redox-Active Rotaxane in a Monolayer Assembly on an Electrode. *J. Am. Chem. Soc.* **2004**, *126*, 15520–15532.
11. Willner, I.; Pardo-Yissar, V.; Katz, E.; Ranjit, K. T. A Photoactivated `Molecular Train' for Optoelectronic Applications: Light-Stimulated Translocation of a β-Cyclodextrin Receptor within a Stoppered Azobenzene-Alkyl Chain Supramolecular Monolayer Assembly on a Au-Electrode. *J. Electroanal. Chem.* **2001**, *497*, 172–177.
12. Nguyen, T. D.; Tseng, H.-R.; Celestre, P. C.; Flood, A. H.; Liu, Y.; Stoddart, J. F.; Zink, J. I. A Reversible Molecular Valve. *Proc. Natl. Acad. Sci. U. S. A.* **2005**, *102*, 10029–10034.
13. Xia, F.; Feng, L.; Wang, S.; Sun, T.; Song, W.; Jiang, W.; Jiang, L. Dual-Responsive Surfaces that Switch Between Superhydrophilicity and Superhydrophobicity. *Adv. Mater.* **2006**, *18*, 432–436.
14. Wang, S.; Song, Y.; Jiang, L. Photoresponsive Surfaces with Controllable Wettability. *Photochem. Photobiol.* **2007**, *8*, 18–29.
15. Cheng, E.; Xing, Y.; Chen, P.; Yang, Y.; Sun, Y.; Zhou, D.; Xu, L.; Fan, Q.; Liu, D. A pH-Triggered, Fast-Responding DNA Hydrogel. *Angew. Chem., Int. Ed.* **2009**, *48*, 7660–7663.
16. Wang, S.; Liu, H.; Liu, D.; Ma, X.; Fang, X.; Jiang, L. Enthalpy-Driven Three-State Switching of a Superhydrophilic/Superhydrophobic Surface. *Angew. Chem., Int. Ed.* **2007**, *46*, 3915–3917.
17. Frasconi, M.; Tel-Vered, R.; Riskin, M.; Willner, I. Electrified Selective "Sponges" Made of Au Nanoparticles. *J. Am. Chem. Soc.* **2010**, *132*, 9373–9382.
18. Serpe, M. J.; Yarmey, K. A.; Nolan, C. M.; Lyon, L. A. Doxorubicin Uptake and Release from Microgel Thin Films. *Biomacromolecules* **2005**, *6*, 408–413.
19. Kanekiyo, Y.; Naganawa, R.; Tao, H. pH-Responsive Molecularly Imprinted Polymers. *Angew. Chem., Int. Ed.* **2003**, *42*, 3014–3016.
20. Riskin, M.; Tel-Vered, R.; Willner, I. Imprinted Au-Nanoparticle Composites for the Ultrasensitive Surface Plasmon Resonance Detection of Hexahydro-1,3,5-trinitro-1,3,5-triazine (RDX). *Adv. Mater.* **2010**, *22*, 1387–1391.
21. Riskin, M.; Tel-Vered, R.; Bourenko, T.; Granot, E.; Willner, I. Imprinting of Molecular Recognition Sites through Electropolymerization of Functionalized Au Nanoparticles: Development of an Electrochemical TNT Sensor Based on π-Donor-Acceptor Interactions. *J. Am. Chem. Soc.* **2008**, *130*, 9726–9733.
22. Zayats, M.; Katz, E.; Baron, R.; Willner, I. Reconstitution of Apo-Glucose Dehydrogenase on Pyrroloquinoline Quinone-Functionalized Au Nanoparticles Yields an Electrically Contacted Biocatalyst. *J. Am. Chem. Soc.* **2005**, *127*, 12400–12406.
23. Yasutomi, S.; Morita, T.; Imanishi, Y.; Kimura, S. A Molecular Photodiode System that Can Switch Photocurrent Direction. *Science* **2004**, *304*, 1944–1947.
24. Doron, A.; Katz, E.; Tao, G.; Willner, I. Photochemically-, Chemically- and pH-Controlled Electrochemistry at Functionalized Spiropyran Monolayer Electrodes. *Langmuir* **1997**, *13*, 1783–1790.
25. Yehezkeli, O.; Moshe, M.; Tel-Vered, R.; Feng, Y.; Li, Y.; Tian, H.; Willner, I. Switchable Photochemical/Electrochemical Wiring of Glucose Oxidase with Electrodes. *Analyst* **2010**, *135*, 474–476.
26. Willner, I.; Katz, E. Magnetic Control of Electrocatalytic and Bioelectrocatalytic Processes. *Angew. Chem., Int. Ed.* **2003**, *42*, 4576–4588.
27. Katz, E.; Baron, R.; Willner, I. Magnetoswitchable Electrochemistry Gated by Alkyl-Chain-Functionalized Magnetic Nanoparticles: Control of Diffusional and Surface-Confined Electrochemical Processes. *J. Am. Chem. Soc.* **2005**, *127*, 4060–4070.
28. Wang, J.; Kawde, A.-N. Magnetic-Field-Stimulated DNA Oxidation. *Electrochem. Commun.* **2002**, *4*, 349–352.
29. Riskin, M.; Tel-Vered, R.; Willner, I. Thermo-Switchable Charge Transport and Electrocatalysis Using Metal-Ion-Modified pNIPAM-Functionalized Electrodes. *Adv. Funct. Mater.* **2009**, *19*, 2474–2480.
30. Tam, T. K.; Pita, M.; Trotsenko, O.; Motornov, M.; Tokarev, I.; Halámek, J.; Minko, S.; Katz, E. Reversible "Closing" of an Electrode Interface Functionalized with a Polymer Brush by an Electrochemical Signal. *Langmuir* **2010**, *26*, 4506–4513.
31. Liu, D.; Bruckbauer, A.; Abell, C.; Balasubramanian, S.; Kang, D.-J.; Klenerman, D.; Zhou, D. A Reversible pH-Driven DNA Nanoswitch Array. *J. Am. Chem. Soc.* **2006**, *128*, 2067–2071.
32. Pardo-Yissar, V.; Gabai, R.; Shipway, A. N.; Bourenko, T.; Willner, I. Gold Nanoparticle/Hydrogel Composites with Solvent-Switchable Electronic Properties. *Adv. Mater.* **2001**, *13*, 1320–1323.
33. Yildiz, H. B.; Tel-Vered, R.; Willner, I. CdS Nanoparticles/β-Cyclodextrin-Functionalized Electrodes for Enhanced

Photoelectrochemistry. *Angew. Chem., Int. Ed.* **2008**, *47*, 6629–6633.
34. Imahori, H.; Yamada, H.; Nishimura, Y.; Yamazaki, I.; Sakata, Y. Vectorial Multistep Electron Transfer at the Gold Electrodes Modified with Self-Assembled Monolayers of Ferrocene-Porphyrin-Fullerene Triads. *J. Phys. Chem. B* **2000**, *104*, 2099–2108.
35. Matsuo, Y.; Ichiki, T.; Nakamura, E. Molecular Photoelectric Switch Using a Mixed SAM of Organic [60] Fullerene and [70] Fullerene Doped with a Single Iron Atom. *J. Am. Chem. Soc.* **2011**, *133*, 9932–9937.
36. Nitahara, S.; Akiyama, T.; Inoue, S.; Yamada, S. A Photoelectronic Switching Device Using a Mixed Self-Assembled Monolayer. *J. Phys. Chem. B* **2005**, *109*, 3944–3948.
37. Yasutomi, S.; Morita, T.; Kimura, S. pH-Controlled Switching of Photocurrent Direction by Self-Assembled Monolayer of Helical Peptides. *J. Am. Chem. Soc.* **2005**, *127*, 14564–14565.
38. Ciesielski, P. N.; Cliffel, D. E.; Jennings, G. K. Kinetic Model of the Photocatalytic Effect of a Photosystem I Monolayer on a Planar Electrode Surface. *J. Phys. Chem. A* **2011**, *115*, 3326–3334.
39. Imahori, H.; Fukuzumi, S. Porphyrin- and Fullerene-Based Molecular Photovoltaic Devices. *Adv. Funct. Mater.* **2004**, *14*, 525–536.
40. Tel-Vered, R.; Yildiz, H. B.; Yan, Y.-M.; Willner, I. Plugging into Enzymes with Light: Photonic "Wiring" of Enzymes with Electrodes for Photobiofuel Cells. *Small* **2010**, *6*, 1593–1597.
41. Sheeney-Haj-Ichia, L.; Wasserman, J.; Willner, I. CdS-Nanoparticle Architectures on Electrodes for Enhanced Photocurrent Generation. *Adv. Mater.* **2002**, *14*, 1323–1326.
42. Tel-Vered, R.; Yehezkeli, O.; Yildiz, H. B.; Wilner., O. I.; Willner, I. Photoelectrochemistry with Ordered CdS Nanoparticle/Relay or Photosensitizer/Relay Dyads on DNA Scaffolds. *Angew. Chem. Int. Ed.,* **2008**, *47*, 8272–8276.
43. Freeman, R.; Liu, X.; Willner, I. Chemiluminescent and Chemiluminescence Resonance Energy Transfer (CRET) Detection of DNA, Metal Ions and Aptamer-Substrate Complexes Using Hemin/G-Quadruplexes and CdSe/ZnS Quantum Dots. *J. Am. Chem. Soc.* **2011**, *133*, 11597–11604.
44. Pardo-Yissar, V.; Bourenko, T.; Wasserman, J.; Willner, I. Solvent-Switchable Photoelectrochemistry in the Presence of CdS-Nanoparticle/Acrylamide Hydrogels. *Adv. Mater.* **2002**, *14*, 670–673.
45. Gill, R.; Patolsky, E.; Katz, E.; Willner, I. Electrochemical Control of the Photocurrent Direction in Intercalated DNA/CdS Nanoparticle Systems. *Angew. Chem.* **2005**, *44*, 4554–4557.
46. Willner, I.; Heleg-Shabtai, V.; Blonder, R.; Katz, E.; Tao, G.; Bückmann, A. F.; Heller, A. Electrical Wiring of Glucose Oxidase by Reconstitution of FAD-Modified Monolayers Assembled onto Au-Electrodes. *J. Am. Chem. Soc.* **1996**, *118*, 10321–10322.
47. Terasaki, N.; Yamamoto, N.; Tamada, K.; Hattori, M.; Hiraga, T.; Tohri, A.; Sato, I.; Iwai, M; Iwai, M.; Taguchi, S.; *et al*. Biophotosensor: Cyanobacterial Photosystem I Coupled with Transistor via Molecular Wire. *Biochim. Biophys. Acta* **2007**, *1767*, 653–659.
48. Terasaki, N.; Yamamoto, N.; Hiraga, T.; Yamanoi, Y.; Yonezawa, T.; Nishihara, H.; Ohmori, T.; Sakai, M.; Fujii, M.; Tohri, A.; *et al*. Plugging a Molecular Wire into Photosystem I: Reconstitution of the Photoelectric Conversion System on a Gold Electrode. *Angew. Chem., Int. Ed.* **2009**, *48*, 1585–1587.
49. Yehezkeli, O.; Wilner, O. I.; Tel-Vered, R.; Roizman-Sade, D.; Nechushtai, R.; Willner, I. Generation of Photocurrents by Bis-aniline-Cross-Linked Pt Nanoparticle/Photosystem I Composites on Electrodes. *J. Phys. Chem. B* **2010**, *114*, 14383–14388.
50. Ciesielski, P. N.; Faulkner, C. J.; Irwin, M. T.; Gregory, J. M.; Tolk, N. H.; Cliffel, D. E.; Jennings, G. K. Enhanced Photocurrent Production by Photosystem I Multilayer Assemblies. *Adv. Funct. Mater.* **2010**, *20*, 4048–4054.
51. Ivanov, B. N. Cooperation of Photosystem I with the Plastoquinone Pool in Oxygen Reduction in Higher Plant Chloroplasts. *Biochemistry (Moscow)* **2008**, *73*, 112–118.
52. Nelson, N.; Nelson, H.; Racker, E. Photoreaction of FMN-Tricine and its Participation in Photophosphorylation. *Photochem. Photobiol.* **1972**, *16*, 481–489.
53. Willner, B.; Katz, E.; Willner, I. Electrical Contacting of Redox Proteins by Nanotechnological Means. *Curr. Opin. Biotech.* **2006**, *17*, 589–596.
54. Kamat, P. V. Photochemistry on Nonreactive and Reactive (Semiconductor) Surfaces. *Chem. Rev.* **1993**, *93*, 267–300.
55. Germano, M.; Yakushevska, A. E.; Keegstra, W.; van Gorkom, H. J.; Dekker, J. P.; Boekema, E. J. Supramolecular Organization of Photosystem I and Light-Harvesting Complex I in Chlamydomonas Reinhardtii. *FEBS Lett.* **2002**, *525*, 121–125.
56. Nechushtai, R.; Muster, P.; Binder, A.; Liveanu, V.; Nelson, N. Photosystem I Reaction Center from the Thermophilic Cyanobacterium Mastigocladus Laminosus. *Proc. Nat. Acad. Sci. U. S. A.* **1983**, *80*, 1179–1183.